

but in no case did any additional features appear or any significant change in band intensity occur.

In all cases the value of *x* (and *y*) quoted refers to the molar ratios of components in the initial mixture from which mixed crystals were made.

Acknowledgment. D.A.K. is indebted to the British Council for financial support.

Registry No. Cr(CO)₆, 13007-92-6; Mo(CO)₆, 13939-06-5; W(CO)₆, 14040-11-0.

References and Notes

- (1) A preliminary account of part of this work has been given: D. A. Kariuki and S. F. A. Kettle, *J. Organomet. Chem.*, **105**, 209 (1976).
- (2) D. M. Adams, W. S. Fernando, and M. A. Hopper, *J. Chem. Soc., Dalton Trans.*, 2264 (1973).
- (3) A. Whitaker and J. W. Jeffrey, *Acta Crystallogr.*, **23**, 977 (1967).
- (4) G. Keeling and P. J. Stamper, Ph.D. Theses, University of Sheffield, 1970.
- (5) R. W. Harrill and H. D. Kaesz, *J. Am. Chem. Soc.*, **90**, 1449 (1968).
- (6) G. Bor and G. Jung, *Inorg. Chim. Acta*, **3**, 69 (1969).
- (7) S. S. Ti, S. F. A. Kettle, and Ø Ra, *Spectrochim. Acta, Part A*, **32a**, 1603 1765 (1976).
- (8) H. J. Hrostowski and G. C. Pimentel, *J. Chem. Phys.*, **19**, 661 (1951).
- (9) D. P. Craig, *Adv. Chem. Phys.*, **8**, 27 (1965).
- (10) A. S. Barker and A. J. Sievers, *Rev. Mod. Phys.*, **47**, S(2)1 (1975).
- (11) H. Takeuchi, I. Harada, and T. Shimanouchi, *Chem. Phys. Lett.*, **43**, 516 (1976).
- (12) R. R. Aggarwal and B. D. Saksena, *J. Chem. Phys.*, **19**, 1480 (1951).
- (13) F. Matossi, *J. Chem. Phys.*, **19**, 161 (1951).
- (14) T. P. Martin, *Phys. Status Solidi B*, **67**, 137 (1975).
- (15) W. Bauhofer, L. Genzel, and I. R. Jahn, *Phys. Status Solidi B*, **63**, 465 (1974).
- (16) P. Dean, *Rev. Mod. Phys.*, **44**, 127 (1972).
- (17) T. Murahashi and T. Koda, *J. Phys. Soc. Jpn.*, **40**, 747 (1976).
- (18) I. Laulicht and R. Ofek, *J. Raman Spectrosc.*, **4**, 41 (1975).
- (19) J. Hoshen and J. Jortner, *J. Chem. Phys.*, **56**, 933 (1972).
- (20) J. B. Bates and H. D. Stidham, *Solid State Commun.*, **16**, 1223 (1975).
- (21) W. Nitsch and R. Claus, *Z. Naturforsch. A*, **29**, 1017 (1974).
- (22) S. S. Ti, Ø Ra, and S. F. A. Kettle, *Spectrochim. Acta, Part A*, **33a**, 111 (1977).
- (23) D. D. Klug and E. Whalley, *J. Chem. Phys.*, **56**, 553 (1972).
- (24) E. Whalley and J. E. Bertie, *J. Chem. Phys.*, **46**, 1264 (1967).
- (25) D. De Fontaine, *J. Appl. Crystallogr.*, **8**, 81 (1975).
- (26) J. H. C. Ching and S. Krimm, *J. Appl. Phys.*, **46**, 4181 (1975).
- (27) J. E. Fergusson and T. W. Tee, *Inorg. Nucl. Chem. Lett.*, **12**, 297 (1976).
- (28) S. L. Barker and S. F. A. Kettle, *Spectrochim. Acta*, in press.
- (29) K. Nakamoto, *Angew. Chem., Int. Ed. Engl.*, **11**, 666 (1972).
- (30) We are indebted to a referee for pointing out that this assignment is in accord with the observation of L. J. Jones, R. S. McDowell, and M. Goldblatt, *Inorg. Chem.*, **8**, 2349 (1969), that band *h* shifts to 1922 cm⁻¹ in Cr(¹³CO)₅ and 1918 cm⁻¹ in Cr(C¹⁸O)₅ demonstrating that it is not to be associated with a mode of Cr(¹²CO)₅(¹³CO). Further these shifts correspond rather well to those observed for the T_{1u} mode, ν₆, in solution.

Contribution from the Department of Inorganic Chemistry, The University, Newcastle upon Tyne, NE1 7RU, England

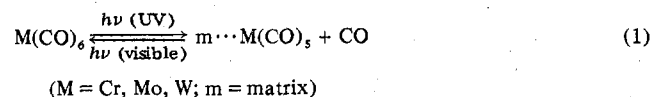
Photolysis and Spectroscopy with Polarized Light: Key to the Photochemistry of Cr(CO)₅ and Related Species¹

JEREMY K. BURDETT, JOSEPH M. GRZYBOWSKI, ROBIN N. PERUTZ, MARTYN POLIAKOFF, JAMES J. TURNER,* and ROBERT F. TURNER

Received April 26, 1977

A photochemical mechanism is proposed which accounts for almost all the experimental data on matrix-isolated M(CO)₅ (M = Cr, Mo, W), N₂M(CO)₅, and M(CO)₅CS. The mechanism is based on evidence obtained by polarized photolysis and polarized spectroscopy of square-pyramidal (spy) L···M(CO)₅ (L = Ar, Xe, N₂ etc.) species. Polarized photolysis of Ar···Mo(CO)₅ in mixed Ar/N₂ matrices leaves oriented Ar···Mo(CO)₅, but the photoproduct N₂Mo(CO)₅ is randomly oriented. Other reactions of this type also exhibit dichroic photodepletion without dichroic photoproduction. In pure matrices polarized photolysis of m···M(CO)₅ (m = matrix) with visible light causes reorientation to positions less favorable to absorption. These results can be understood from a three-step mechanism consisting of (1) photochemical ejection of the sixth ligand m from spy m···M(CO)₅, (2) internal rearrangements of the resulting naked M(CO)₅ via a trigonal-bipyramidal (tbp) intermediate and decay back to the spy ground state in one of several orientations, (3) recombination with an alternative ligand, CO, Ar, N₂ etc. This spy → tbp → spy process represents an inverse Berry mechanism and also accounts for many other aspects of the photochemistry (e.g., recombination with CO to M(CO)₆). A similar mechanism also explains the initial formation of M(CO)₅ from M(CO)₆. The details of the mechanism are developed from an assignment of the photochemically active absorption and from molecular orbital arguments using both extended Hückel and angular overlap methods.

On ultraviolet photolysis of metal hexacarbonyls of chromium, molybdenum, and tungsten in low-temperature matrices, CO and square-pyramidal metal pentacarbonyls are generated. Irradiation of the pentacarbonyl in its visible absorption band results in the reversal of this reaction (eq 1).²



The infrared and UV/visible spectra and the photochemical properties of the metal pentacarbonyls have been studied under a wide variety of conditions.²⁻⁷ These experiments and those on the analogous system M(CO)₅CS (M = Cr, W)^{8,9} have been summarized in a recent review.¹⁰ In this paper we describe in detail the additional information obtained by using polarized photolysis and detection (a short communication was published

earlier¹¹). We use a molecular orbital treatment to suggest a photochemical pathway which accounts for almost all the data, both new and old.

I. Experiments with Polarized Light

Although the use of polarized photolysis and detection in low-temperature glasses was described many years ago,¹² the technique is still new for matrix isolation.¹¹ A detailed analysis of other applications of the method and a description of the experimental technique will be given elsewhere.¹³

If a nonrotating molecule (of lower symmetry than cubic) is photolyzed with plane-polarized light in a matrix, the preferential absorption of the photolyzing light by molecules in some orientations will lead to partial orientation of the remaining starting material (*dichroic photodepletion*). If there were no rotation in the photochemical reaction, the product would be preferentially oriented in the opposite direction

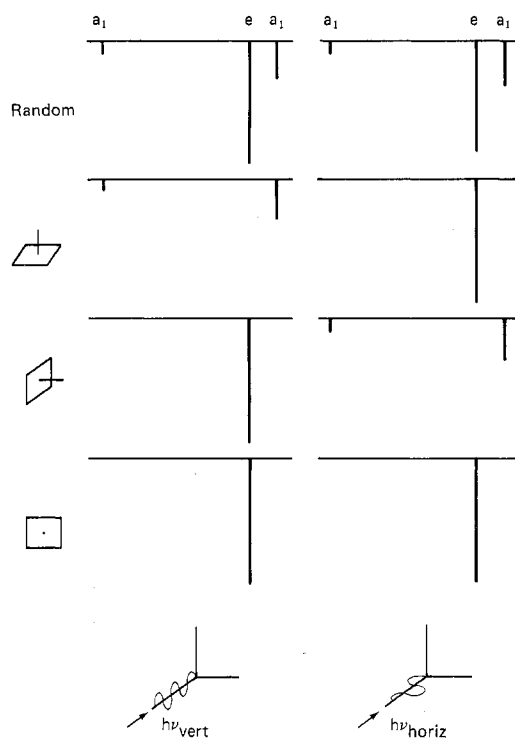


Figure 1. Schematic representation of the relationship between polarization of light and IR absorption of $M(CO)_5$ or $N_2M(CO)_5$ in three extreme orientations in the CO stretching region.

Table I. Proportionalities for Absorption of Polarized Light^a

Transition moment			
Symmetry	Direction	A_{vert}^b	A_{horiz}^b
a_1	z'	$B \cos^2 \theta$	$B \sin^2 \theta \sin^2 \phi$
e	x', y'	$B' \sin^2 \theta$	$B'(\cos^2 \theta \sin^2 \phi + \cos^2 \phi)$

^a Adapted from ref 12 (Albrecht's papers). ^b A values are proportional to absorbance, B and B' are absorption cross sections. ^c x', y', z' and θ, ϕ are defined in Figure 2.

(*dichroic photoproduction*). A third phenomenon is possible if the starting material rotates after absorption but does not react. Preferential orientation then results with little or no depletion (*photoreorientation*). All three phenomena may be detected by infrared and UV/visible spectroscopy using polarized light.

In our experiments a carbonyl sample, very dilute in the matrix gas, is deposited as a film on a flat spectroscopic window held in the vertical plane and photolyzed with light perpendicular to the window.¹⁴ IR and UV/visible spectra are recorded with light incident in the same direction. When plane-polarized light is used for photolysis or detection, this will be represented as $h\nu_{\text{vert}}$ if the electric vector is vertical and $h\nu_{\text{horiz}}$ if the vector is horizontal. The effect of polarized light on absorption can be visualized by considering the hypothetical IR spectra of $C_{4v} M(CO)_5$ in three extreme orientations (Figure 1) (the IR-active CO stretching modes transform as $2a_1 + e$, while the x, y, z axes transform as $e + a_1$). More quantitatively, the probability of absorption by a single molecule is given by the proportionalities in Table I (axes defined by Figure 2).^{12,15} The behavior of a real sample, which will not reach the extremes of Figure 1, may be calculated from the sum of the individual molecular contributions given by these proportionalities.

II. Polarized Photochemistry of $M(CO)_5/N_2M(CO)_5$ in Mixed Matrices

A mixture of $Ar \cdots Mo(CO)_5$ and $N_2Mo(CO)_5$ was generated by unpolarized UV photolysis of $Mo(CO)_6$ in a mixed

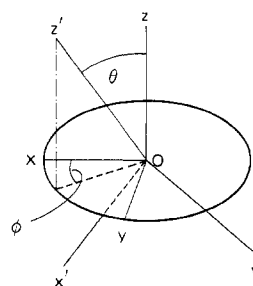


Figure 2. Molecule with molecule-fixed axes x', y', z' held rigid in matrix with space-fixed axes x, y, z . Light incident along x axis can be polarized with electric vector along z (vertical) or y (horizontal) axis (adapted from ref 15).

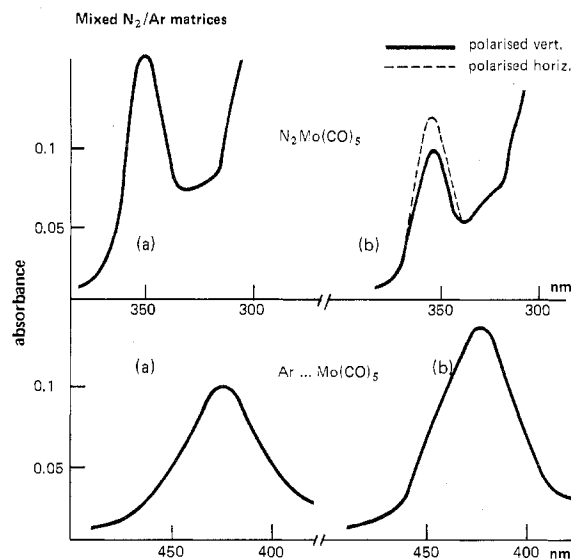
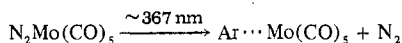


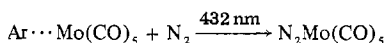
Figure 3. UV/visible spectrum obtained after UV photolysis of $Mo(CO)_6$ in a mixed Ar/N_2 (1:1) matrix after (a) 30 min of unpolarized photolysis with $\lambda \sim 314$ nm and (b) 45-min photolysis with $\lambda \sim 367$ nm, $h\nu_{\text{vert}}$: (—) spectrum polarized vertically, (---) spectrum polarized horizontally.

N_2/Ar matrix ($Mo(CO)_6:Ar:N_2 = 1:1000:1000$) at 20 K.^{10,16,17} It was then photolyzed with plane-polarized light ($\lambda \approx 367$ nm) in order to promote the reaction



The UV/visible spectra of both $N_2Mo(CO)_5$ and $Ar \cdots Mo(CO)_5$ are initially identical for the two polarizer orientations ($A_{\text{vert}} = A_{\text{horiz}}$) indicating the random orientation of the sample (Figure 3a). On polarized photolysis the $N_2Mo(CO)_5$ absorption develops dichroism (Figure 3b) indicating partial orientation. On the other hand the $Ar \cdots Mo(CO)_5$ increases in intensity but remains randomly oriented. The orientation of the $N_2Mo(CO)_5$ is expected according to the theory of dichroic photodepletion (see above). The lack of orientation of the product $Ar \cdots Mo(CO)_5$ demonstrates that there is motion during the reaction, which prevents the observation of dichroic photoproduction.¹³ These effects are found both in the IR and UV spectra in mixed N_2/Ar and N_2/CH_4 matrices.

When the reverse reaction



is promoted with polarized light, it is the $Ar \cdots Mo(CO)_5$ which becomes partially oriented, while the $N_2Mo(CO)_5$ remains randomly oriented. Thus we are again observing dichroic photodepletion without dichroic photoproduction. The reactions are summarized in Table II. As has been observed

Table II. Polarized Photolysis of Ar...Mo(CO)₅ and N₂Mo(CO)₅

Photolysis wavelength, nm	Ar...Mo(CO) ₅ ^a	N ₂ Mo(CO) ₅ ^a
367	R throughout	R → O
432	R → O	R throughout

^a Key: R = random, O = oriented.

Table III. Absorbances of Visible Band (λ_{max} ~489 nm) of CH₄...Cr(CO)₅ in Pure CH₄ Following Polarized Visible Photolysis (λ >375 nm)

Polarization	Photolysis time, ^a min	Absorbance	
		Horiz	Vert
Unpol	0	0.28	0.28
Vert	1	0.28	0.25
Horiz	25	0.21	0.28
Vert	10	0.25	0.19

^a These times refer to sequential photolyses in the same experiment.

in other matrix reactions, there must be some motion during the photochemical act which randomizes the orientation of the photoproduct.¹³

III. Polarized Photolysis in Pure Matrices

When a sample of CH₄...Cr(CO)₅, generated by unpolarized UV photolysis of Cr(CO)₆ in pure CH₄, is photolyzed with $h\nu_{\text{vert}}$ (λ >375 nm), the visible spectrum shows developing linear dichroism in the CH₄...Cr(CO)₅. On further photolysis with $h\nu_{\text{horiz}}$ the dichroism observed in the spectrum is reversed. A second reversal may be induced by photolyzing again with $h\nu_{\text{vert}}$.¹¹ The absorbances measured in these experiments show that each reversal is accompanied by an increase in optical density of one polarization relative to the previous spectrum (Table III). Similar results were obtained by photolyzing N₂Cr(CO)₅ in pure N₂ (Figure 4) or Ar...Cr(CO)₅ in pure Ar, in the appropriate visible band. In all these experiments any dichroism is destroyed by photolyzing with unpolarized light.

The linear dichroism in these spectra indicates preferential orientation of m...Cr(CO)₅ (m = matrix), just as in the experiments in mixed matrices. Each time the sample of Cr(CO)₅ is photolyzed with visible light there is some conversion to Cr(CO)₆. However, the increase in intensity of one polarization demonstrates that the molecules are being re-oriented to positions where they have a lower probability of absorbing the incident radiation. This is the phenomenon of photoreorientation mentioned in section I as the third possible effect of polarized photolysis. It can be observed here because the rate of reorientation is comparable to that of recombination. In the experiments in mixed matrices the higher rate of reaction precluded the detection of photoreorientation.

The preferential orientation of a sample may be detected both in the IR and in the UV/visible spectra.¹¹

Since the symmetry of the CO stretching modes is known,³ the symmetry of the transition moments for the UV/visible bands may be deduced. The behavior of the longest wavelength UV/visible absorptions of both M(CO)₅ and N₂M(CO)₅ mirrors that of the IR bands of species e and is the opposite to those of species a₁ (see ref 3). Thus the longest wavelength UV/visible absorption bands must have a transition moment of species e. The consistency of the polarization data with the photochemical activity of these bands may be tested by comparing the polarization of the absorption with that used for photolysis. As expected it is A_{vert} which decreases fastest on photolysis with $h\nu_{\text{vert}}$.

The symmetry of the visible band may be used to specify the spatial orientation (relative to laboratory axes) of the oriented samples. With $h\nu_{\text{vert}}$, m...Cr(CO)₅ accumulates with the fourfold axis vertical. This process of turning over of

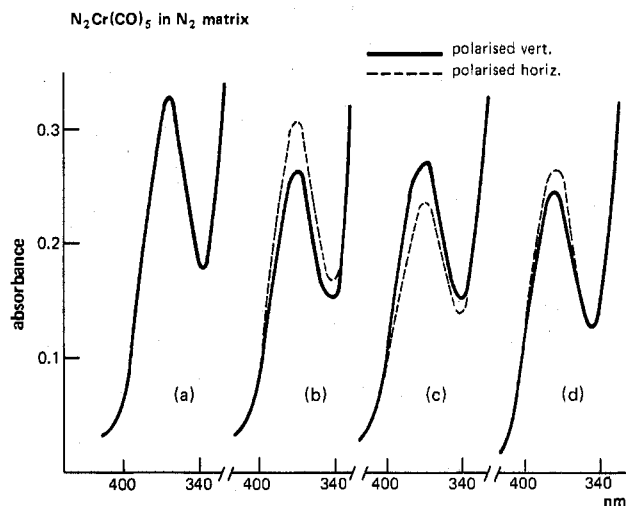
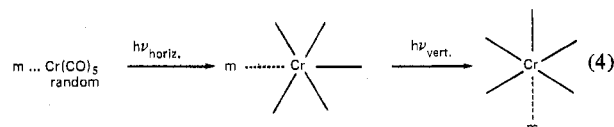


Figure 4. Effect of polarized photolysis on the near-UV absorption of N₂Cr(CO)₅ in pure N₂ (a) after 20 min of unpolarized photolysis of Cr(CO)₆ in N₂, λ ~314 nm, and photolysis with λ ~367 nm, (b) with $h\nu_{\text{vert}}$, 20 min, (c) with $h\nu_{\text{horiz}}$, 30 min, and (d) with $h\nu_{\text{vert}}$, 15 min: (—) spectrum polarized vertically, (---) spectrum polarized horizontally.

m...Cr(CO)₅ on polarized visible irradiation is illustrated in eq 4. Although this process might be expected to continue

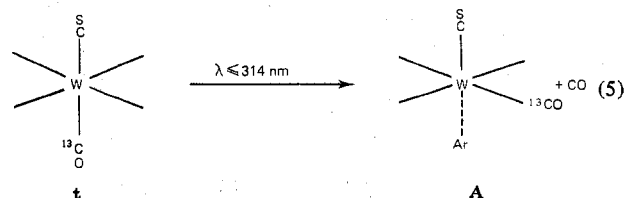


until the sample was completely oriented (a dichroic ratio¹⁸ of 1), we have never observed a dichroic ratio in excess of 0.15. This can be attributed both to the symmetry species of the absorption bands and to the imperfections of our spectral setup.¹³ It should be noted that the matrix may be kept indefinitely without loss of dichroism, and it may even be annealed to temperatures above 40 K without affecting the degree of polarization. Further experiments in which dichroic samples were annealed are discussed in section V.

The ability to maintain oriented samples demonstrates the lack of fluxionality of the ground state of d⁶ M(CO)₅ at these temperatures. Fe(CO)₅, a molecule which is still fluxional at 100 K, can also be preferentially oriented in a matrix.¹⁹ By analogy, d⁶ M(CO)₅ could be fluxional in its ground electronic state at higher temperatures even though it is rigid at 20 K.

IV. Polarization Experiments with W(CO)₅CS

When W(CO)₅CS is photolyzed in matrices, W(CO)₄CS is generated in two isomeric forms, with the CS group occupying either axial or equatorial positions of a square-pyramidal structure. Isomerization of the M(CO)₄CS can be induced by selective photolysis.⁸ As described earlier⁸ photolysis of M(CO)₅CS with plane-polarized light (λ ~300 nm) leaves an oriented sample of unreacted M(CO)₅CS. This represents an example of dichroic photodepletion in the reaction to lose CO from the six-coordinate starting material. Stereospecifically labeled *trans*-(¹³C)W(CO)₄CS has been used to demonstrate⁹ that isomerization is an integral step in the photochemical generation of W(CO)₄CS (eq 5). The



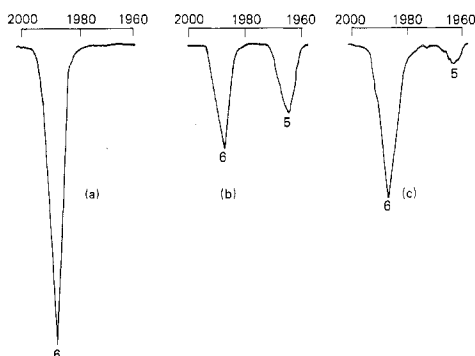


Figure 5. Annealing behavior. IR spectra of $W(CO)_6$ in SF_6/CO (20:1) (a) at 20 K, (b) after 10 min of photolysis with $\lambda \sim 230 \text{ nm}$ —5 $\equiv W(CO)_5$, and (c) after warming to 40 K for 8 min and recooling to 20 K.

isomerization was shown to take place in an excited state of the fragment, i.e., after ejection of CO and not in the parent molecule.

In order to clarify the processes occurring in this reaction we photolyzed a sample of *trans*- $(^{13}CO)W(CO)_4CS$ (**t**) with polarized light ($\lambda < 314 \text{ nm}$, see eq 3, ref 9). As expected, **t** remaining after photolysis showed considerable linear dichroism. Unlike the reactions of $N_2M(CO)_5$ there was a reproducible but smaller orientation of the product $Ar \cdots (^{13}CO)W(CO)_3CS$ (**A**) in the opposite direction (i.e., the a'' mode of **A** had the opposite polarization to the e mode of **t**). The sample was then irradiated with unpolarized visible light ($\lambda > 375 \text{ nm}$). No trace of dichroism was found in the IR bands of the regenerated *cis*- $(^{13}CO)W(CO)_4CS$ (**e**) even though the bands of **t** still remained polarized after irradiation.

The smaller polarization of the product **A** than of the starting material **t** shows that dichroic photoproduction was incomplete. Therefore, UV photolysis of **t** not only causes a change in the relative positions of the ^{13}CO and CS groups from *trans* to *cis* but also a substantial rotation of either the CS or the ^{13}CO groups relative to the laboratory axes. The randomization of the final product **e** implies that a further rotation takes place during the recombination with CO.

V. Thermal Behavior of $M(CO)_5$

When $M(CO)_5$ is generated in pure Ar matrices, it is *not* observed to recombine with CO on warming the matrix to 40 K. However, if the matrix is doped with a few percent CO, some of the $M(CO)_5$ recombines with CO on annealing.²³ The polarization experiments suggest that the *photochemical* recombination of $M(CO)_5$ with CO is associated with reorientation of $M(CO)_5$ in the matrix (see below). On annealing an oriented sample, no loss of polarization is observed (section III). These observations lead to the hypothesis that the lack of recombination of $M(CO)_5$ in pure Ar is related to the inability of $M(CO)_5$ to reorient at 40 K. In order to test this theory, we have studied the thermal behavior of $M(CO)_5$ in SF_6 matrices which have a much larger annealing range than Ar.

Figure 5 shows the results of experiments involving the photochemical generation of $W(CO)_5$ in SF_6 followed by annealing. Recombination with CO occurs whether or not the matrix is doped with excess CO, but it is much faster in CO-doped matrices. We have also generated $Cr(CO)_5$ in a PVC film doped with THF at 77 K. Warming the film to $120 \pm 20 \text{ K}$ resulted in the smooth conversion of $Cr(CO)_5$ into $Cr(CO)_6$ and $Cr(CO)_5 \cdot THF$.

Generation of oriented samples of $W(CO)_5$ in SF_6 was hampered by rapid photochemical regeneration of $W(CO)_6$. However, oriented samples did not appear to lose dichroism when thermal recombination began. The implication of these

and previous experiments is that thermal recombination requires a suitably positioned CO molecule and that there is *no* reorientation of the fragment before recombination.

VI. Mechanistic Consequences of the Experiments

The polarization experiments have demonstrated the motion inherent in the photochemical act occurring on visible irradiation of $m \cdots M(CO)_5$. The association between facile photochemical recombination and changes in the orientation of $M(CO)_5$ may be contrasted with the reluctance of $M(CO)_5$ to undergo thermal recombination with CO or thermal reorientation. According to the mechanism described in the first paper in this series,² the photochemical recombination of $M(CO)_5$ with CO is a thermal effect caused by the production of a local hot spot around the absorbing molecule. The CO diffuses in the resulting "local soup" and recombines with the carbonyl fragment. Since the publication of that paper, both theoretical^{20,21} and experimental evidence have become available showing that any excess energy is dissipated very rapidly with minimal disturbance of the cage. In particular, Brus and Bondybey²² have examined emission from ICl in matrices and shown that "there is no evidence for a transient local "hot spot" of well defined temperature".

Many of the observations on $M(CO)_5$ and $M(CO)_4CS$ described earlier could be explained by local heating if the local temperatures were in excess of 80 K. However, in view of the evidence against a hot spot, alternative mechanisms must be examined.²³

In two-component mixed matrices two $M(CO)_5$ species are observed corresponding to stereospecific interaction of $M(CO)_5$ with one or other component through the sixth coordination position (e.g., $Ar \cdots M(CO)_5$ and $N_2M(CO)_5$ in Ar/N_2 matrices). These two species can be interconverted by selective visible photolysis.^{4,10} These ligand exchange experiments strongly suggest that the sixth ligand of $LM(CO)_5$ ($L = Ar, N_2$ etc.) is photochemically ejected and that this ligand is then replaced by another one. The isomerization of $M(CO)_4CS$ indicates that the photochemical act involves an internal rearrangement,^{8,9} while the polarization results require a rotation (either real or apparent) of the carbonyl molecule. These requirements can be accommodated in the following three-step mechanism: (a) expulsion of L from $LM(CO)_5$ ($L = Ar, N_2$ etc.); (b) internal rearrangement of $M(CO)_5$, resulting in axial-equatorial ligand exchange and an apparent rotation; (c) recombination with a sixth ligand L' to give $L'M(CO)_5$ ($L' = CO, Ar, N_2$ etc.).

So far we have discussed only the photolysis of $LM(CO)_5$, $m \cdots M(CO)_5$, and related species. However, the photolysis of $M(CO)_6$ and $M(CO)_5CS$ also poses mechanistic problems in the initial escape of the ejected CO and the rearrangement of the ^{13}CO and CS labeled molecule, eq 5. There is no inherent reason why the initial loss of CO should proceed by the same mechanism as that for the reverse reaction, since different electronic states may be involved. Nevertheless, we favor a more complete mechanism than simple diffusion of the escaping CO in a local hot spot because (a) the CO does not escape from the cage on initial photolysis³ and (b) the photolysis of *trans*- $(^{13}CO)W(CO)_4CS$ ⁹ involves an internal rearrangement. The evidence is consistent with a three-step process analogous to that proposed above with $L = CO$.

VII. Assignment of the UV/Visible Spectrum of $m \cdots M(CO)_5$ and Its Consequences

In this section and the next we turn to molecular orbital arguments to define the pathway more closely. The validity of the first step of the proposed mechanism (ligand expulsion) can be tested from the assignment of the visible band of $M(CO)_5$ and by comparison with the behavior of $LM(CO)_5$ complexes in solution. The d-orbital splitting diagram for $C_{4v} M(CO)_5$ is illustrated in Figure 6a.²⁴ We have shown above

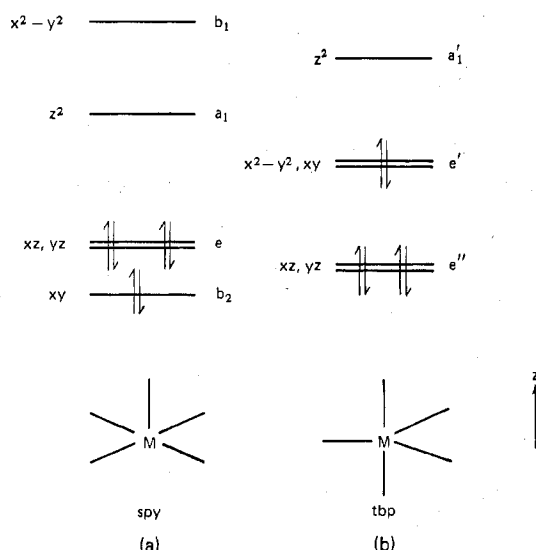


Figure 6. d orbital splitting diagrams for (a) square-pyramidal (spy) and (b) trigonal-bipyramidal (tbp) M(CO)₅ (d⁶).

that the transition moment for the visible band has species e symmetry. This is consistent with the assignment of the band to the $e \rightarrow a_1$ (d_{z^2}) transition, which has been adopted by us for the matrix species⁴ and by most authors for stable LM(CO)₅ complexes.^{25,26} It is not, however, conclusive proof, since both the $e \rightarrow b_1$ and some components of the $e \rightarrow \pi^*$ CO transitions also have e symmetry.

The assignment of the longest wavelength band of LM(CO)₅ complexes which are stable at room temperature to the $e \rightarrow a_1$ transition is justified as follows. Irradiation of these complexes in solution in this band leads to loss of either L or CO, with a much higher quantum yield for loss of L than for CO.²⁵ Loss of L is expected on population of the a_1 (d_{z^2}) orbital since the greatest antibonding character of this orbital is associated with the ligand L rather than the CO ligands.²⁴ In contrast, population of the b_1 ($d_{x^2-y^2}$) orbital should lead to expulsion of equatorial CO because of the M-C σ -antibonding character in the xy plane. Since the π^* CO orbitals are probably M-C bonding, CO loss is not expected for CO charge-transfer states.²⁷ Thus irradiation into band A must lead to population of the a_1 (d_{z^2}) orbital either directly or by internal conversion. That direct population occurs has been proved by some elegant experiments of Wrighton et al.²⁸

The long-wavelength band of the matrix-isolated $m \cdots M$ (CO)₅ (m = matrix) complex corresponds in wavelength, intensity, and photochemistry to that of stable LM(CO)₅ complexes. Thus it may safely be assigned to the $e \rightarrow a_1$ (d_{z^2}) transition (¹A \rightarrow ¹E). We infer that such excitation leads directly to truly naked M(CO)₅, which then undergoes an internal rearrangement in the next step of the mechanism.

The behavior of $m \cdots M$ (CO)₅ (m = matrix) on short-wavelength excitation can also be understood on this ligand field model. On irradiation into the $M \rightarrow \pi^*$ CO charge-transfer band²⁹ at about 245 nm, both CO loss and recombination with CO are observed. The photoreactions probably result from internal conversion to ligand field states with population of the $d_{x^2-y^2}$ orbital leading to loss of equatorial CO or population of the d_{z^2} orbital leading to loss of M and recombination with CO. Stable LM(CO)₅ complexes also show an increasing quantum yield for CO loss at shorter wavelengths.^{25,29}

VIII. Electronic Structure of M(CO)₅ and Internal Rearrangements

Both Burdett³⁰ and Elian and Hoffmann²⁴ have reported the analysis of numerous binary metal carbonyl geometries

Table IV. d-Orbital Stabilization Energies^a of M(CO)₅ (units of $\beta_\sigma S_\sigma^2$)

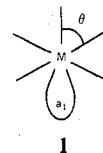
Configuration	M	Orbital occupation no. ^b	tbp	spy	C_{2v} ^c
d ⁶ low spin	Cr	22 200	7.75	10	8
d ⁶ intermediate spin	Cr	22 110	7.75	8	7.75
d ⁷ low spin	Mn	22 210	6.625	8	6.75
d ⁸ low spin	Fe	22 220	5.5	6	5.5

^a Calculated from the angular overlap model.³² ^b The number of electrons in each d orbital, working upward in energy, e.g., for spy Cr(CO)₅ (see Figure 6) d⁶ low spin is " $b_2^2 e^2 e^2$ " and d⁶ intermediate spin is " $b_1^2 e^2 e^2 a_1$ ". ^c Structure as in (7) (see later).

by extended Hückel MO calculations with gratifyingly similar results. Veillard et al.³¹ have reported ab initio calculations on V(CO)₅, Mn(CO)₅, and Fe(CO)₅, and very recently have examined Cr(CO)₅ itself. Burdett³² has also examined the geometries of such systems in terms of competition between a d-orbital stabilization energy favoring a square-pyramidal (spy geometry) and the repulsion forces favoring a trigonal-bipyramidal (tbp) geometry. Encouragingly, this angular overlap model, the two sets of extended Hückel calculations, and the ab initio calculations agree in predicting a spy geometry for d⁶ M(CO)₅ in the singlet ground state. Here we use both new and published MO results to examine the plausibility of the mechanism and to predict the structure of electronically excited M(CO)₅.

Table IV shows the d-orbital stabilization energies obtained from the angular overlap model for three five-coordinate geometries (see ref 32). The argument may be illustrated using d⁸ Fe(CO)₅ and d⁶ Cr(CO)₅ as examples. Although the stabilization energy for Fe(CO)₅ favors a spy geometry, the margin of stability over the tbp structure is so small ($0.5 \beta_\sigma S_\sigma^2$) that the repulsion forces cause adoption of the tbp geometry. For Cr(CO)₅ the substantial margin by which the spy geometry is favored ($2.25 \beta_\sigma S_\sigma^2$) is sufficient to stabilize the molecule in this geometry.

The MO analyses also account for much of the behavior of d⁶ spy M(CO)₅. The lowest three d orbitals (see Figure 6a) are primarily involved in π bonding. The LUMO is mainly σ antibonding; in addition to d_{z^2} character, it contains a significant contribution from the $(n+1)s$ and $(n+1)p_z$ metal orbitals. Elian and Hoffmann have shown that this a_1 orbital protrudes from the base of the square pyramid and has an ideal shape and energy to act as an acceptor orbital for interaction with the sixth ligand (1). Thus it is not surprising to find that



Cr(CO)₅ is so sensitive to interaction with the matrix material via this site.^{4,10} On the other hand, this interaction is certainly too small to be the principal cause of the preference for a spy rather than a tbp geometry (e.g., the $Ne \cdots Cr(CO)_5$ interaction energy must be extremely small).

Three sets of authors^{24,30,33} have shown independently that the relative energy of the d orbitals in these spy systems is very sensitive to the droop angle, θ , of the molecule (1). All agree that the $e \rightarrow a_1$ energy separation increases as the angle decreases from 100 to 90°. We have found evidence for an increase in this angle from $Xe \cdots Cr(CO)_5$ to $Ar \cdots Cr(CO)_5$.^{4,10} Accordingly we have attributed the extreme sensitivity of the position of the visible band of M(CO)₅ to a combination of (a) a direct bonding interaction with the a_1 orbital and (b) a decrease in the droop angle. Both these effects act in concert

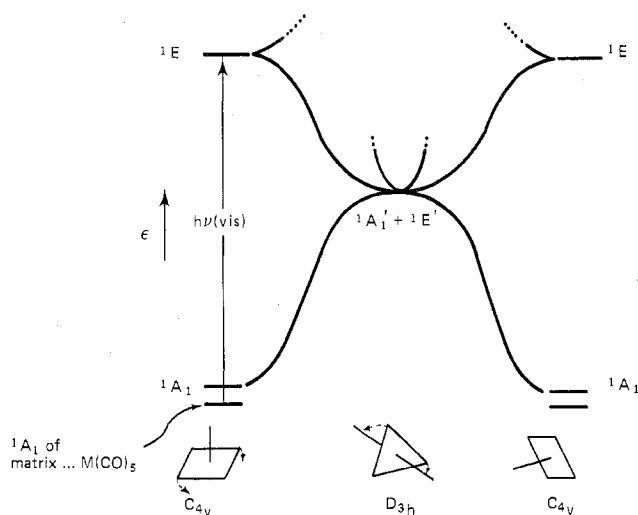


Figure 7. Energy diagram for the ground and first excited singlet states of a d^6 $M(\text{CO})_5$ fragment, a slice through the potential energy surface connecting square-pyramidal and trigonal-bipyramidal geometries. (N.B. There are in fact three possible spy permutations connecting with each tbp.)

to increase the separation of the e and a_1 orbitals. Thus these considerations are entirely consistent with the assignment of the visible absorption band given above



The geometry of d^6 $M(\text{CO})_5$ in its first excited singlet state may be predicted to be tbp from Table IV (d^6 , 22 110). It is unlikely to be square pyramidal, since the stabilization of this geometry over tbp ($0.25 \beta_p S_p^2$) is less than that for $\text{Fe}(\text{CO})_5$, which is known to adopt the tbp geometry. We have confirmed by extended Hückel calculations that this configuration should have an energy minimum at the tbp structure. However, within the singlet manifold this electronic structure (tbp: $(e'')^4(e')^2$, see Figure 6b) correlates with both the ground and first excited states of the C_{4v} geometry. Thus the energy profiles for distortion of the ground and first excited singlet states of the C_{4v} structure touch at the D_{3h} configuration (Figure 7). This effect can also be seen in terms of two Jahn-Teller instabilities. The 1E C_{4v} configuration is unstable with respect to the D_{3h} geometry, but the $^1E'$ D_{3h} configuration is unstable with respect to the C_{4v} structure again. Figure 7 only shows the correlation of the *lower* components of the degenerate pairs for the 1E and $^1E'$ states of the two structures. The partners of these states correlate with higher energy states which do not concern us here. The figure is strikingly similar to the Renner-Teller description³⁴ of the ground and first excited electronic states of NH_2 and other triatomic hydrides with quasi-linear first excited electronic states which become equienergetic at the linear geometry ($^2\Pi$). The geometry of the first excited singlet of d^6 $M(\text{CO})_5$ may be described as quasi-trigonal bipyramidal.

Since the MO methods used above do not distinguish different spin states, the first excited singlet and triplet states are predicted to have the same energy. However, the triplet state with tbp geometry ($^3A_2'$) is stable with respect to the spy geometry.³¹ Its energy profile is described by the upper curve of Figure 7.

The analysis of the geometry of the first excited singlet state of d^6 $M(\text{CO})_5$ enables us to trace a possible photochemical pathway for $X \cdots M(\text{CO})_5$ following visible excitation. In the ground state the molecule is trapped in potential wells of spy geometry; it neither rotates nor undergoes internal rearrangements in the low-temperature matrix. On visible excitation the sixth ligand X (Ar, N_2 , etc.) is ejected and the

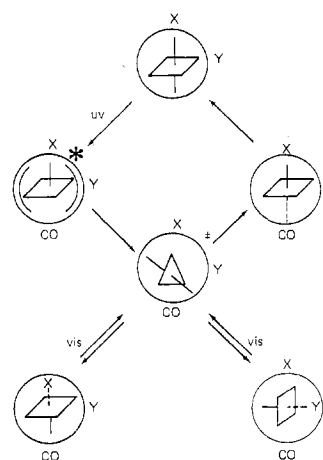


Figure 8. Photochemical behavior of " $M(\text{CO})_5$ " in a mixed matrix containing X, Y. Reorientation via a trigonal-bipyramidal intermediate. (Each rotation of the spy should strictly be 120° , not 90° ; 90° angles are used here for simplicity.) Key: *, electronically excited state; +, electronically or vibrationally excited state.

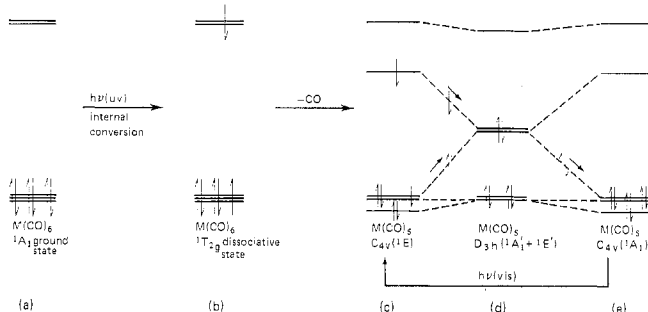


Figure 9. Molecular orbital counterpart of Figure 8, showing production and visible excitation of $M(\text{CO})_5$.

molecule is placed in a highly vibrationally excited state centered at the tbp geometry. It runs "downhill" to the D_{3h} structure and then to one of the ground-state C_{4v} structures where it picks up the same or a different ligand. The details of the energy-transfer process must await the results of further studies.

IX. Photochemistry Linking $M(\text{CO})_6$ and $M(\text{CO})_5$

We are now in a position to propose a more complete account of the photochemical behavior of these species. A scheme compatible with the observations and making use of the molecular orbital arguments is depicted in Figure 8 in two-dimensional form. The MO counterpart of the scheme is shown in Figure 9. The hexacarbonyl trapped in the cage of a matrix containing X and Y atoms loses a CO molecule after UV irradiation leaving a spy $M(\text{CO})_5$ molecule which we shall assume to be in an excited electronic state. (We further assume for the present that this is the first excited singlet state, although the argument is unaffected if it is a triplet—see section X.) The spy geometry is unstable for this electronic configuration and the molecule distorts to the tbp geometry. The tbp geometry connects with three possible ground-state spy molecules to which it has an equal chance of proceeding. One of them has a spatial orientation such that a Y atom is adjacent to the sixth site, one contains an X atom in this position, and the third has the same orientation as the electronically excited spy molecule produced initially. In the first two environments the CO molecule is not situated advantageously for recombination with the carbonyl fragment and $Y \cdots M(\text{CO})_5$ and $X \cdots M(\text{CO})_5$ result. In the third orientation facile recombination with CO may occur to give the hexacarbonyl.

This mechanism requires that the loss of CO from $\text{M}(\text{CO})_6$ should be accompanied by an excited-state rearrangement of the $\text{M}(\text{CO})_5$ fragment. It is unusual for photochemical cleavage to yield products in an excited state, but in the closely analogous $\text{M}(\text{CO})_5\text{CS}$ system, such a rearrangement has been shown to occur in a vibrationally or electronically excited state of the photoproduct $\text{M}(\text{CO})_4\text{CS}$.⁹

The route from $\text{M}(\text{CO})_6$ to $\text{M}(\text{CO})_5$ accounts for the escape of the ejected CO from the sixth site of $\text{M}(\text{CO})_5$ without leaving the cage itself. The maximum quantum yield for the production of $m\cdots\text{M}(\text{CO})_5$ is predicted to be two-thirds, exactly equal to the value recently measured for $\text{Cr}(\text{CO})_6$ in cyclohexane solution (0.67)!³⁵ The route also shows how *trans*-(^{13}CO) $\text{W}(\text{CO})_4\text{CS}$ can be photolyzed to yield *cis*-(^{13}CO)- $\text{W}(\text{CO})_3\text{CS}$ as principal product.⁹ The rearrangement takes place in the five-coordinate excited state via a process equivalent to the inverse Berry twist (see below).

Visible irradiation of $Y\cdots\text{M}(\text{CO})_5$ populates the *tbp* geometry which may then give $\text{M}(\text{CO})_6$ (recombination) or $X\cdots\text{M}(\text{CO})_5$ (mixed-matrix ligand exchange, section II) or $Y\cdots\text{M}(\text{CO})_5$ again. The photochemical recombination with CO will be facile if the rearrangement brings the sixth site of $\text{M}(\text{CO})_5$ close to the CO molecule ejected initially. The photoreorientation process (section III) on visible photolysis is seen as a consequence of the internal rearrangement; no physical rotation is required, only the pseudorotation through 120° inherent in the *spy* \rightarrow *tbp* \rightarrow *spy* interconversion (the inverse Berry twist).^{36,37} The photochemically induced isomerization⁸ of $\text{M}(\text{CO})_4\text{CS}$ is another manifestation of the inverse Berry twist, which effects an axial-equatorial ligand exchange. The maximum quantum yield for recombination should be one-sixth, only one-quarter the value for the initial production of $\text{M}(\text{CO})_5$. The ratio of the quantum yield for production of $\text{Mo}(\text{CO})_5$ to that for recombination to $\text{Mo}(\text{CO})_6$ has been measured in Ar, CH_4 , and CO matrices.⁷ Although the value for Ar matrices agrees exactly with the predicted value (0.25), that for CH_4 is quite different (0.04). Indirect evidence suggests intermediate values for other rare gas matrices. The reasons for the differences are thought to reflect the rates of deactivation of excited $\text{M}(\text{CO})_6$ and $\text{M}(\text{CO})_5$ but are not understood in detail.

The scheme shown in Figure 8 has been simplified for two-dimensional display. In fact, two *tbp* molecules are accessible from each *spy* molecule, depending on which pair of radial ligands is depressed. By an inverse Berry twist, one particular square pyramid may connect with a number of other orientations, a conclusion which explains the randomization of the photoproducts of oriented $\text{Ar}\cdots\text{Mo}(\text{CO})_5$ and $\text{N}_2\cdots\text{Mo}(\text{CO})_5$ (section II). The implication of this mechanism for the photochemistry of $\text{M}(\text{CO})_6$ in solution is discussed elsewhere.¹⁰

The proposed mechanism involves an effective rotation of the $\text{M}(\text{CO})_5$ fragment. It might be argued that such a motion is surprising in a "rigid" matrix at low temperature and that the matrix plays a more important role in the course of the reaction than we have suggested. In considering these arguments the following points should be noted. (i) The effective rotation produced by the *spy* \rightarrow *tbp* \rightarrow *spy* interconversion involves only very small movements of the carbonyl groups. The process occurs during the photochemical act; subsequently, the molecule is held rigid, at least up to the boil-off temperature of the matrix. (ii) There are no authenticated examples known to us, in which matrix rigidity forces a gross change in structure relative to an unperturbed situation. (iii) Some recent experiments have illustrated the role of the cage in matrix reactions.^{22,38} On the one hand, the high compressibility of the matrix allows the cage to accommodate changes in guest size incurred by photolysis (e.g., the change

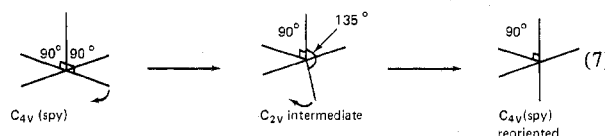
in equilibrium bond distance of ICl in an excited state or the expulsion of CO from $\text{M}(\text{CO})_6$). Such *adiabatic* changes are possible with very little influence of the host on the movements of the guest, because the vibrations of the host are separated in time scale from movements of the guest (a sort of Born-Oppenheimer approximation). On the other hand, *impulsive* collisions of guest atoms with host atoms can prevent permanent photodissociation, leading to in-cage recombination and the familiar cage effect. Brus and Bondybey observed both phenomena in the single example of ICl in Ar lattices.³⁸ Finally it is important that the cage does not in general allow rotation of the guest even in the presence of excess energy. For instance, polarized stimulation of emission of ICl in Ar showed that negligible angular reorientation accompanies the photodissociation-recombination process, even for excitation 0.8 eV above the relevant dissociation barrier. Thus although the reorientation of $m\cdots\text{M}(\text{CO})_5$ is not unique,^{13,19} excess energy will not necessarily lead to rotation in the lattice.

X. Alternative Mechanisms

We showed earlier that the *photothermal* mechanism was highly implausible; are there any other alternatives to the scheme put forward in sections VIII and IX?

The scheme of Figure 9 was drawn so as to involve singlet excited states only. A variant on the mechanism involves the triplet manifold of $\text{M}(\text{CO})_5$ and $\text{M}(\text{CO})_6$. If Figure 9 is redrawn in the triplet manifold, it will be qualitatively unchanged except that (i) the unpaired electrons in (b) and (c) have parallel spins as do the highest energy pair of electrons in (d) and (ii) there is no smooth progression from (d) to (e). Instead there will be simple T_1 to S_0 relaxation. Thus overall the observed photochemistry is expected to be identical in both manifolds. However, no increase in photosensitivity is observed on moving from $\text{Cr}(\text{CO})_5$ to $\text{W}(\text{CO})_5$, as would be expected if the triplet route were significant.³⁹

Relaxation of a D_{3h} structure can occur in three ways to give differently oriented ground-state C_{4v} geometries. Application of Stanton and McIver's rules⁴⁰ shows that thermal interconversion between these C_{4v} ground-state geometries cannot have the D_{3h} configuration as the transition state although it can be an intermediate—there must be a lower energy pathway. Our calculations suggest that this transition state has C_{2v} geometry with bond angles 90 , 135 , and 135° (eq 7).



For clarity the distortion coordinate in eq 7 is shown as movement of a single ligand; in practice there will be an overall rotation counter to the ligand movement to maintain zero net angular momentum. Table IV shows that the d-orbital stabilization energy of this geometry for low-spin d^6 $\text{M}(\text{CO})_5$ lies between that for the *spy* and *tbp* geometries. For the other electronic configurations of Table IV, the d-orbital stabilization energy of the new geometry is the same as for the *tbp*, so the repulsion forces will make the structure disfavored. These results which are confirmed by extended Hückel calculations⁴¹ are shown in Figure 10. Thermally, but not photochemically, the process in (7) should be favored relative to the *tbp* pathway for low-spin d^6 $\text{M}(\text{CO})_5$ (i.e., the ground electronic state of the carbonyl). This equatorial-hole exchange mechanism belongs to the same observable process category as the *spy* equivalent of the Berry process described above,³⁷ and thus it is difficult to detect experimentally.

All the mechanisms considered so far in this paper have involved dissociative replacement of L in $\text{LM}(\text{CO})_5$ by L' . Although we consider an associative *photochemical* mechanism

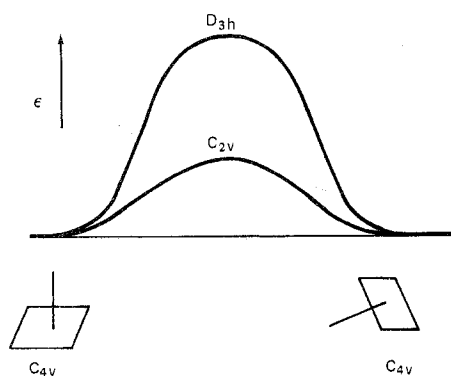


Figure 10. Distortion coordinate for spy $M(CO)_5$ via C_{2v} intermediate (eq 7) and tbp intermediate (D_{3h}) in the ground electronic state of $d^6 M(CO)_5$.

to be implausible, associative reactions could occur during annealing (see section V).

XI. Other Applications of the Photochemical Mechanism

The photochemical mechanism described in section IX suggests that reorientation of the $M(CO)_5$ inherent in the photochemical act allows the escape of the ejected CO from the vacant site. Photochemical yields in other systems may also be strongly influenced by electronic effects on the relative orientation of the products. Sometimes a lack of reorientation may cause immediate recombination, reducing the observed product yield drastically. Possible examples are the low yield for CO loss from the tetrahedral molecules $Ni(CO)_4$ and $Fe(CO)_2(NO)_2$ ⁴² and the lack of $Mn(CO)_5$ from $Mn_2(CO)_{10}$.⁴² In other situations, the reorientation of products may enhance the yield even when a strong cage effect might have been anticipated. For instance, despite its size, pyridine can be expelled photochemically from $W(CO)_5(py)$ in Ar matrices.⁴³

Registry No. $Mo(CO)_5$, 32312-17-7; $Cr(CO)_5$, 26319-33-5; $Fe(CO)_5$, 13463-40-6; $W(CO)_5$, 30395-19-8; $Mn(CO)_5$, 15651-51-1; $Mo(CO)_6$, 13939-06-5; $W(CO)_6$, 14040-11-0; $Cr(CO)_6$, 13007-92-6; $N_2Mo(CO)_5$, 64364-80-3; $N_2Cr(CO)_5$, 34416-63-2.

References and Notes

- (1) This research was supported by the S.R.C.
- (2) M. A. Graham, M. Poliakoff, and J. J. Turner, *J. Chem. Soc. A*, 2939 (1971).
- (3) R. N. Perutz and J. J. Turner, *Inorg. Chem.*, **14**, 262 (1975).
- (4) R. N. Perutz and J. J. Turner, *J. Am. Chem. Soc.*, **97**, 4791 (1975).
- (5) R. N. Perutz and J. J. Turner, *J. Am. Chem. Soc.*, **97**, 4800 (1975).
- (6) J. K. Burdett, R. N. Perutz, M. Poliakoff, A. J. Rest, J. J. Turner, and R. F. Turner, *J. Am. Chem. Soc.*, **97**, 4805 (1975).
- (7) M. Poliakoff, *J. Chem. Soc., Faraday Trans. 2*, **72**, 569 (1977).

- (8) M. Poliakoff, *Inorg. Chem.*, **15**, 2022 (1976).
- (9) M. Poliakoff, *Inorg. Chem.*, **15**, 2892 (1976).
- (10) J. K. Burdett, R. N. Perutz, M. Poliakoff, and J. J. Turner, *Pure Appl. Chem.*, **49**, 271 (1977).
- (11) J. K. Burdett, R. N. Perutz, M. Poliakoff, and J. J. Turner, *J. Chem. Soc., Chem. Commun.*, 157 (1975).
- (12) G. N. Lewis and D. Lipkin, *J. Am. Chem. Soc.*, **64**, 2801 (1942); G. N. Lewis and J. Bigeleisen, *ibid.*, **65**, 520 (1943); A. C. Albrecht, *J. Mol. Spectrosc.*, **6**, 84 (1961); A. C. Albrecht, *J. Chem. Phys.*, **27**, 1413 (1957).
- (13) J. K. Burdett, I. R. Dunkin, J. M. Grzybowski, M. Poliakoff, and J. J. Turner, to be submitted for publication.
- (14) The experimental details for handling the metal carbonyls are as given in ref 4.
- (15) E. B. Wilson, J. C. Decius, and P. C. Cross, "Molecular Vibrations", McGraw-Hill, New York, N.Y., 1955.
- (16) M. A. Graham, Ph.D. Thesis, University of Cambridge, 1971.
- (17) R. F. Turner, Ph.D. Thesis, University of Newcastle upon Tyne, 1976.
- (18) Dichroic ratio = $(A_v - A_h)/(A_v + A_h)$ (v = vertical, h = horizontal).
- (19) J. K. Burdett, J. M. Grzybowski, M. Poliakoff, and J. J. Turner, *J. Am. Chem. Soc.*, **98**, 5728 (1976).
- (20) J. K. Burdett and J. J. Turner in "Cryogenic Chemistry", M. Moskovitz and G. A. Ozin, Ed., Wiley, New York, N.Y., 1976.
- (21) J. K. Burdett, unpublished work; H. Coufal, private communication.
- (22) V. E. Bondybey and L. E. Brus, *J. Chem. Phys.*, **64**, 3724 (1976).
- (23) Originally,² the behavior of the matrix splittings of $M(CO)_6$ was adduced as evidence in favor of the photothermal theory. However, they have recently been shown to be caused by multiple trapping rather than distortion. Thus the changes in the splitting patterns observed on photolysis represent changes in the occupation of sites rather than relief of distortion (R. N. Perutz, Ph.D. Thesis, University of Cambridge, 1974).
- (24) M. Elian and R. Hoffmann, *Inorg. Chem.*, **14**, 1058 (1975).
- (25) M. Wrighton, *Chem. Rev.*, **74**, 401 (1974).
- (26) R. A. N. McLean, *J. Chem. Soc., Dalton Trans.*, 1568 (1974).
- (27) P. S. Braterman, "Metal Carbonyl Spectra", Academic Press, New York, N.Y., 1975.
- (28) M. S. Wrighton, H. B. Abrahamson, and D. L. Morse, *J. Am. Chem. Soc.*, **98**, 4105 (1976).
- (29) A ligand field assignment for the UV band can be excluded because of both its energy and intensity. No bands corresponding to direct population of the d_{z^2} orbital are observed for $M(CO)_5$, but they have been found for some stable $LW(CO)_5$ complexes.²⁵
- (30) J. K. Burdett, *J. Chem. Soc., Faraday Trans. 2*, **70**, 1599 (1974).
- (31) A. Veillard, private communication; J. Demnynck, A. Strick, and A. Veillard, *Nouv. J. Chim.*, in press. See also P. J. Hay, Abstracts, American Chemical Society Meeting, Fort Worth, Tex., 1976.
- (32) J. K. Burdett, *Inorg. Chem.*, **14**, 375 (1975).
- (33) D. Guenzburger, A. O. Caride, and E. Zuleta, *Chem. Phys. Lett.*, **14**, 239 (1972).
- (34) See for example G. Herzberg "Electronic Spectra of Polyatomic Molecules", Van Nostrand-Reinhold, New York, N.Y., 1966.
- (35) J. Nasielski and A. Colas, *J. Organomet. Chem.*, **101**, 215 (1975).
- (36) R. S. Berry, *J. Chem. Phys.*, **32**, 933 (1960).
- (37) J. I. Musher and W. C. Agosta, *J. Am. Chem. Soc.*, **96**, 1320 (1974).
- (38) L. E. Brus and V. E. Bondybey, *J. Chem. Phys.*, **65**, 71 (1976), and personal communication.
- (39) Spin-orbit coupling should increase the intersystem crossing rate to the triplet manifold.
- (40) R. E. Stanton and J. W. McIver, *J. Am. Chem. Soc.*, **97**, 3632 (1975). These rules forbid transition states with threefold axes.
- (41) Similar results are obtained whether the parametrization of Burdett³⁰ or of Elian and Hoffmann²⁴ is used.
- (42) O. Crichton and A. J. Rest, *J. Chem. Soc., Dalton Trans.*, 656 (1977).
- (43) A. J. Rest and J. Sodeau, *J. Chem. Soc., Chem. Commun.*, 696 (1975).